Supporting Information

Hydrophilic Packaging of Iron Oxide Nanoclusters for Highly Sensitive Imaging

Cartney E. Smith, Dawn Ernenwein, Artem Shkumatov,

Nicholas Clay, JuYeon Lee, Molly Melhem, Sanjay Misra,

Steven C. Zimmerman, and Hyunjoon Kong

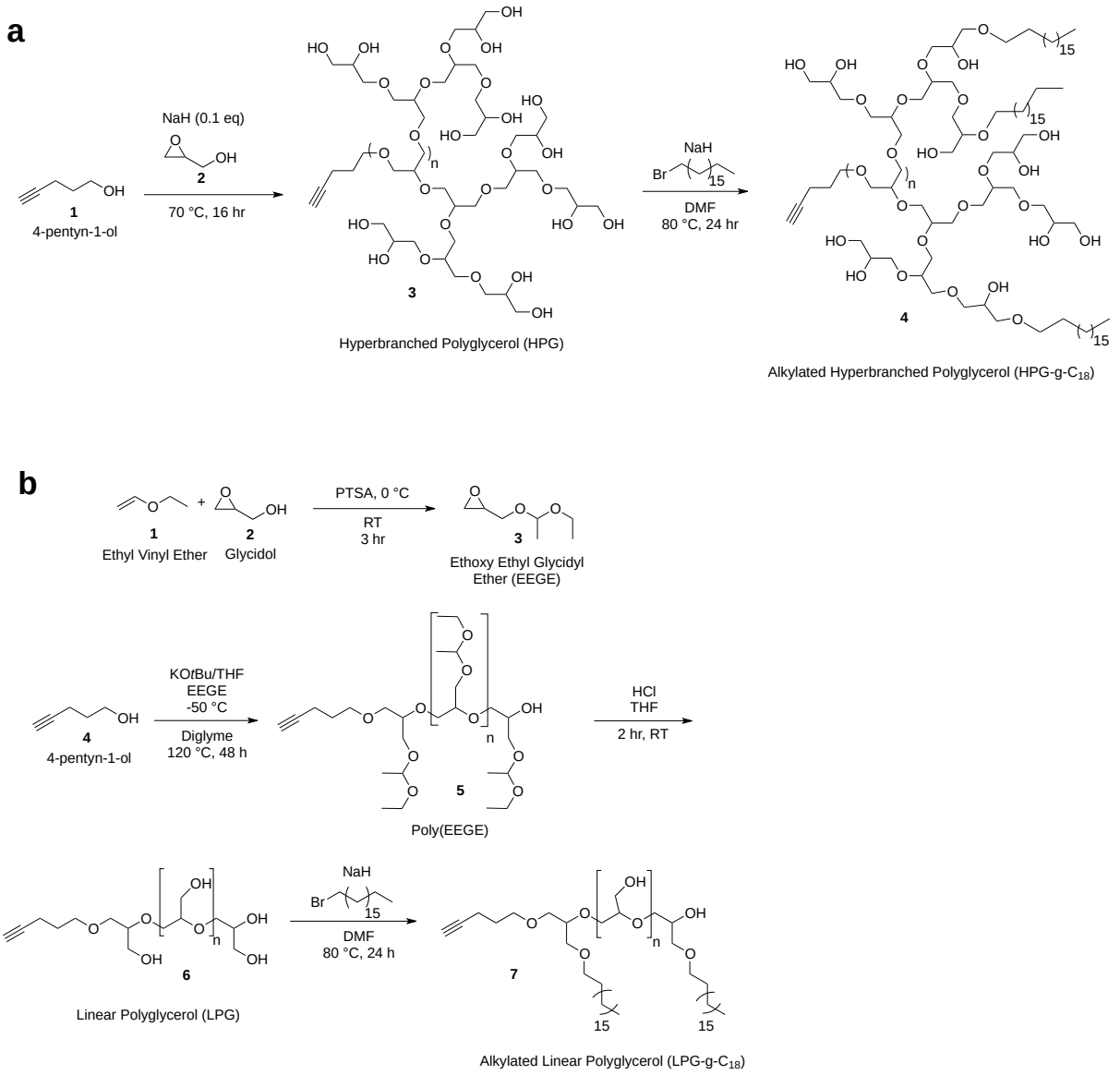

Figure S1. Synthesis of **(a)** alkylated HPG and **(b)** alkylated LPG.

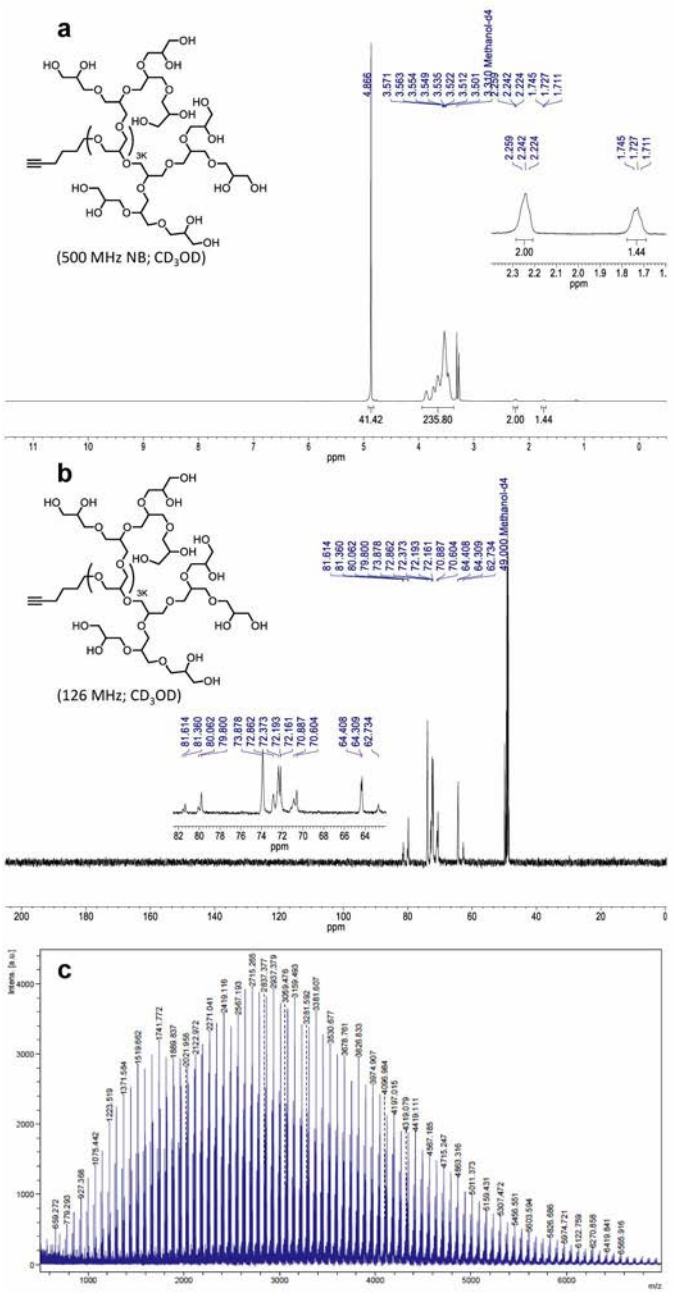

Figure S2. Characterization of HPG_{3k} by **(a)** ^{1}H NMR, **(b)** ^{13}C NMR, and **(c)** MALDI-TOF. HPG_{3k} represents HPG with a molecular weight (MW) of 3,000 g/mol. **^{1}H NMR** (400 MHz, methanol-d_4) δ 4.87 (s, 41H), 3.94 – 3.37 (m, 236H), 2.24 (t, J = 7.0 Hz, 2H), 1.78 – 1.69 (m, 1H). **^{13}C NMR** (126 MHz, methanol-d_4) δ 81.61, 81.36, 80.06, 79.80, 73.88, 72.86, 72.37, 72.19, 72.16, 70.89, 70.60, 64.41, 64.31, 62.73. **MS (MALDI)** m/z ~3000, peak separation 74 m/z units.

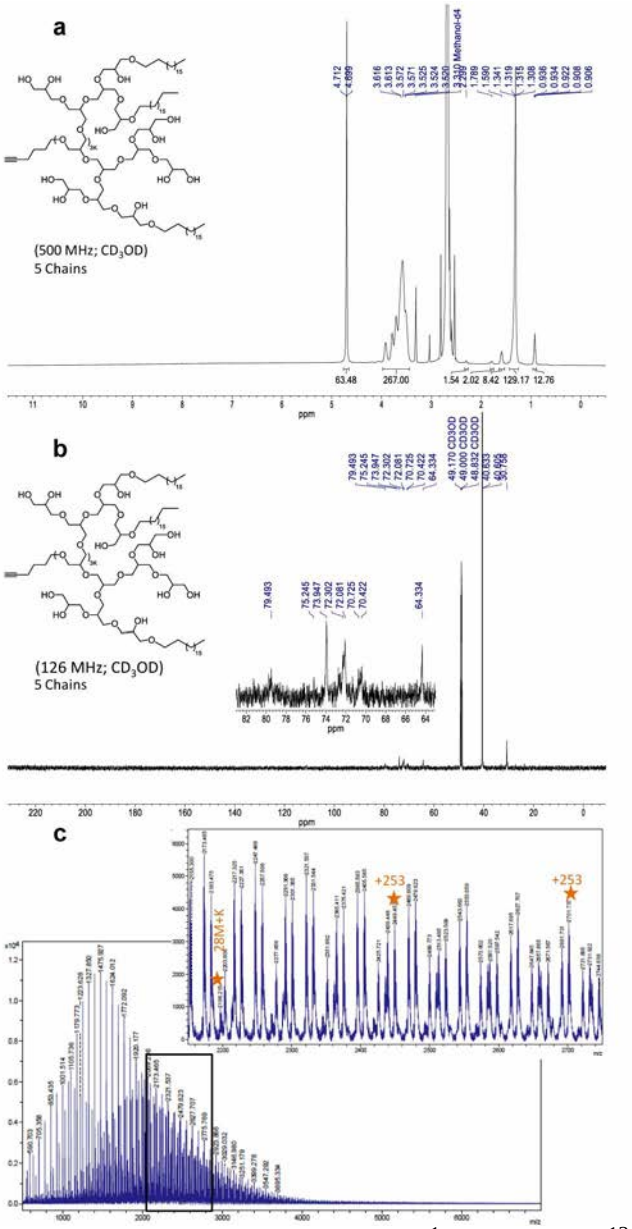

Figure S3. Characterization of HPG_{3k}-g-C_{18}(5) by **(a)** ^{1}H NMR, **(b)** ^{13}C NMR, and **(c)** MALDI-TOF. Protons of the C_{18} chain are from 1-2 ppm in the ^{1}H NMR spectrum. HPG_{3k}-g-C_{18}(5) represents HPG (MW ~3,000 g/mol) substituted with 5 C_{18} chains. **^{1}H NMR** (500 MHz, methanol-d_4) δ 4.71 (d, J = 6.6 Hz, 63H), 3.97 – 3.44 (m, 267H), 2.30 (s, 2H), 1.79 (s, 2H), 1.59 (s, 8H), 1.43 – 1.25 (m, 129H), 0.96 – 0.89 (m, 13H). **^{13}C NMR** (126 MHz, methanol-d_4) δ 79.49, 73.95, 72.30, 72.08, 70.73, 70.42, 64.33, 40.63, 40.61, 30.76. **MS (MALDI)** peak separation 253 m/z units.

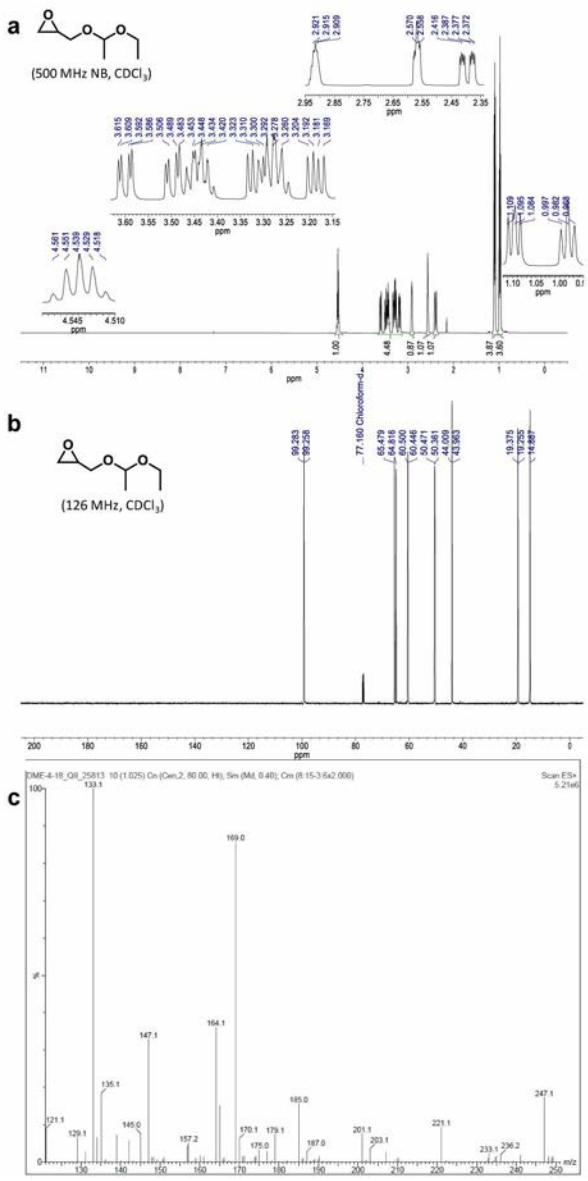

Figure S4. Characterization of EEGE, an LPG synthetic intermediate, by **(a)** ^{1}H NMR, **(b)** ^{13}C NMR, and **(c)** ESI mass spectrometry, calculated 146 m/z, experimental 147.1 (M+1), 169.0 m/z (M+Na). **^{1}H NMR** (500 MHz, chloroform-*d*) δ 4.58 – 4.49 (m, 1H), 3.64 – 3.14 (m, 5H), 2.95 – 2.88 (m, 1H), 2.57 (ddt, *J* = 5.9, 3.1, 1.5 Hz, 1H), 2.43 – 2.35 (m, 1H), 1.10 (ddd, *J* = 6.5, 5.4, 1.1 Hz, 4H), 0.98 (tt, *J* = 7.1, 1.3 Hz, 4H). **^{13}C NMR** (126 MHz, chloroform-*d*) δ 99.28, 99.26, 65.48, 64.82, 60.50, 60.45, 50.47, 50.36, 44.01, 43.96, 19.37, 19.25, 14.89.

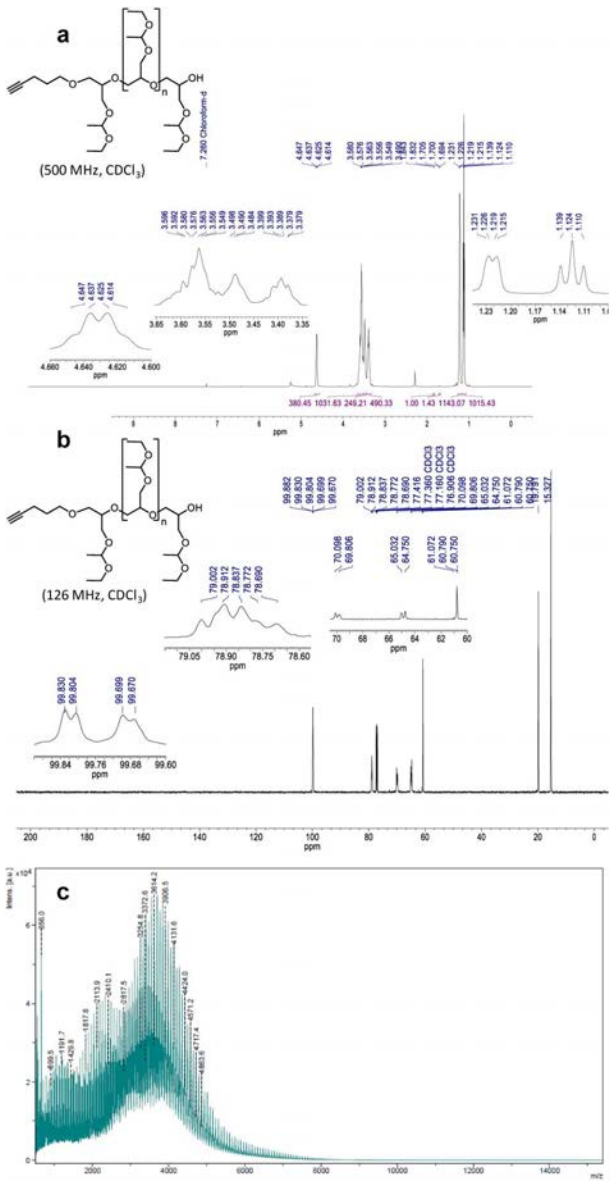

Figure S5. Characterization of poly(EEGE), an LPG synthetic intermediate, by **(a)** ^{1}H NMR, **(b)** ^{13}C NMR, and **(c)** MALDI-TOF. **^{1}H NMR** (500 MHz, chloroform-*d*) δ 4.63 (q, *J* = 5.5 Hz, 380H), 3.65 – 3.51 (m, 1032H), 3.49 (q, *J* = 4.2 Hz, 249H), 3.44 – 3.34 (m, 490H), 1.84 (d, *J* = 5.6 Hz, 1H), 1.70 (t, *J* = 2.6 Hz, 1H), 1.26 – 1.18 (m, 1143H), 1.12 (t, *J* = 7.1 Hz, 1015H). **^{13}C NMR** (126 MHz, $CDCl_3$) δ 99.88, 99.83, 99.80, 99.70, 99.67, 79.00, 78.91, 78.84, 78.77, 78.69, 77.42, 70.10, 69.81, 65.03, 64.75, 62.38, 61.07, 61.02, 60.79, 60.75, 19.79, 15.33. **MS (MALDI)** 3600 m/z, peak separation of 147 m/z units.

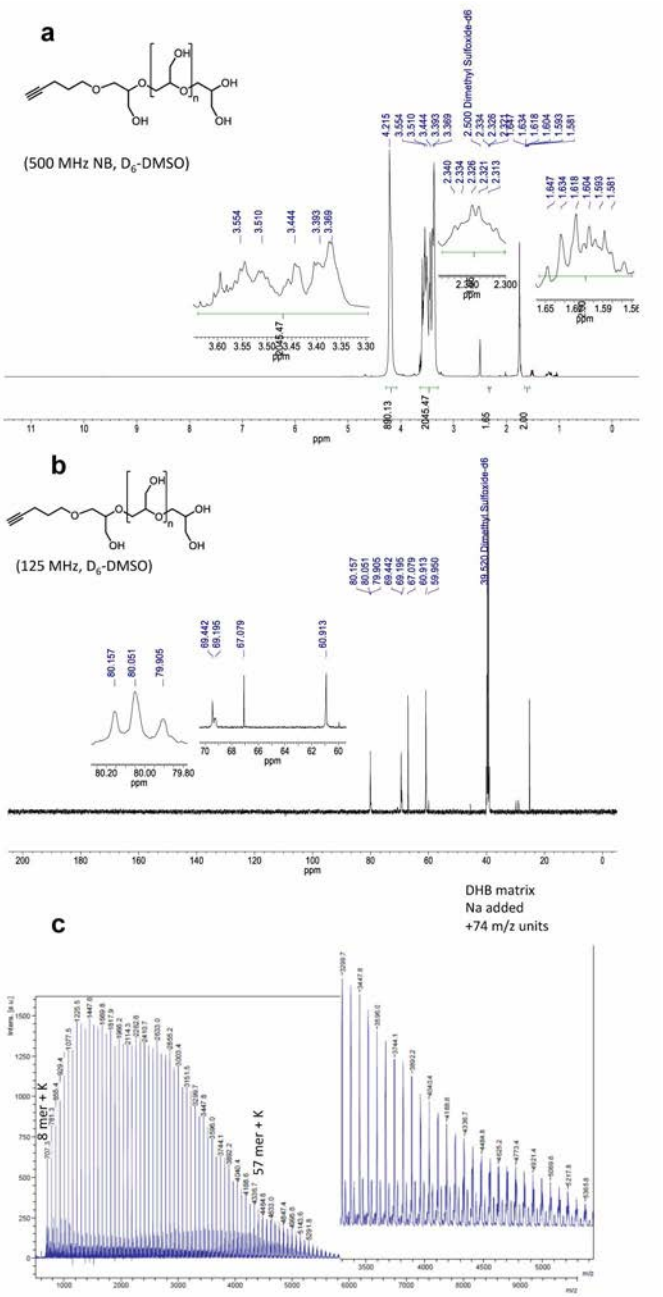

Figure S6. Characterization of LPG_{3k} by **(a)** ^{1}H NMR, **(b)** ^{13}C NMR, and **(c)** MALDI-TOF. LPG_{3k} represents LPG with MW of ~3,000 g/mol. **^{1}H NMR** (500 MHz, DMSO-d_6) δ 4.29 – 4.11 (m, 1044H), 3.62 – 3.32 (m, 1897H), 2.32 (td, J = 6.9, 3.0 Hz, 1H), 1.65 – 1.58 (m, 2H). **^{13}C NMR** (126 MHz, DMSO-d_6) δ 80.16, 80.05, 79.91, 69.45, 69.29, 67.08, 60.92, 59.95, 40.02, 39.94, 39.86, 39.78, 39.69, 39.60, 39.52, 39.35, 39.27, 39.19, 39.02. **MS (MALDI)** ~3000 m/z, separation of 74 m/z units.

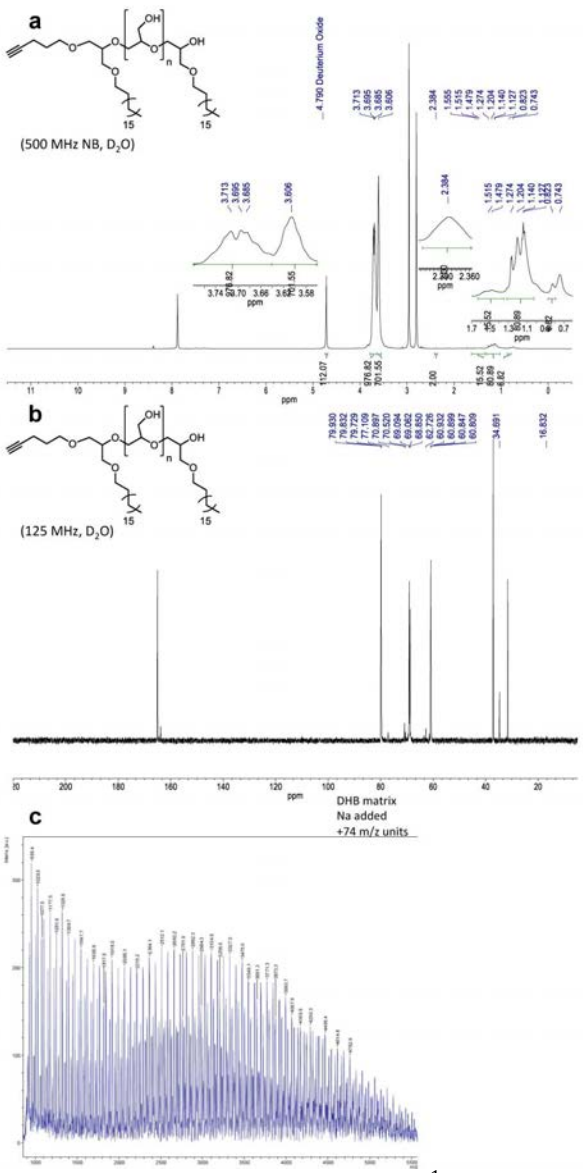

Figure S7. Characterization of LPG_{3k}-g-C_{18}(2) by **(a)** ^{1}H NMR, **(b)** ^{13}C NMR, and **(c)** MALDI-TOF. Protons of the C_{18} chain are from 1-2 ppm in the ^{1}H NMR spectrum. LPG_{3k}-g-C_{18}(2) represents LPG (MW ~3,000 g/mol) substituted with 2 C_{18} chains. **^{1}H NMR** (500 MHz, deuterium oxide) δ 3.70 (dd, *J* = 15.5, 9.7 Hz, 977H), 3.61 (s, 702H), 2.38 (s, 2H), 1.52 (m, 16H), 1.24 – 0.98 (m, 80H), 0.77 (s, 6H). **^{13}C NMR** (127 MHz, deuterium oxide) δ 79.93, 79.83, 79.73, 77.11, 70.90, 70.52, 69.09, 69.06, 68.85, 62.73, 60.93, 60.90, 60.85, 60.81, 37.08, 34.69, 31.57, 16.83. **MS (MALDI)** ~3500 m/z, separation of 74 m/z units.

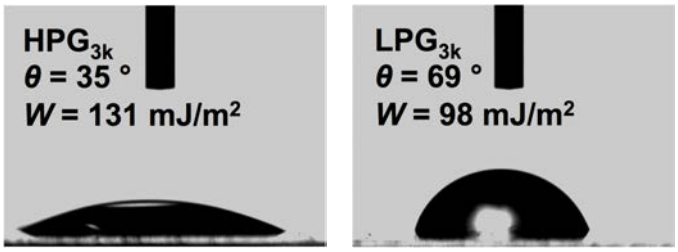

Figure S8. Contact angles and corresponding surface energies of water droplets on films of HPG_{3k} and LPG_{3k}.

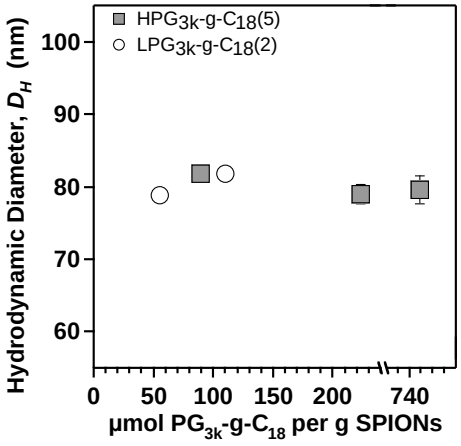

Figure S9. Z-average hydrodynamic diameter of SPION nanoclusters produced by various concentrations of HPG_{3k}-g-C_{18}(5) (■) and LPG_{3k}-g-C_{18}(2) (○). HPG_{3k}-g-C_{18}(5) and LPG_{3k}-g-C_{18}(2) represent HPG substituted with 5 C_{18} chains and LPG substituted with 2 C_{18} chains, respectively. Molecular weights of both HPG and LPG were 3,000 g/mol. Error bars, though partially obscured by data point markers, represent standard deviation of three measurements.

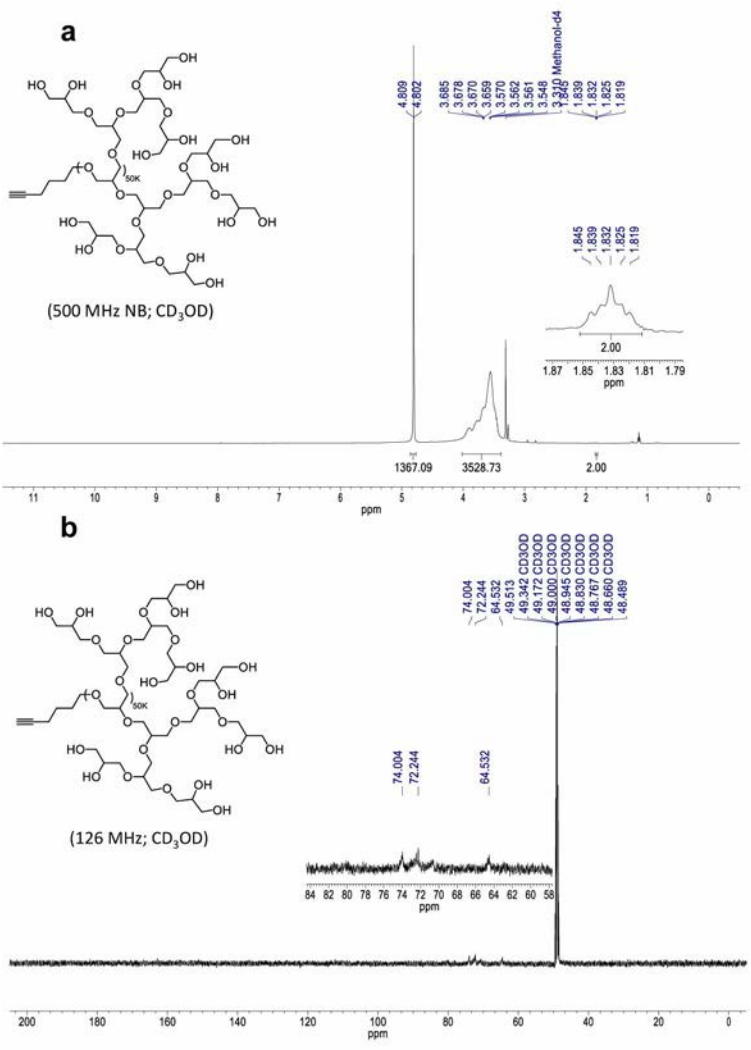

Figure S10. Characterization of HPG_{50k} by **(a)** ^{1}H NMR and **(b)** ^{13}C NMR. HPG_{50k} represents HPG with MW of ~50,000 g/mol. **^{1}H NMR** (500 MHz, methanol-d_4) δ 4.86 – 4.77 (m, 1367H), 4.02 – 3.39 (m, 3529H), 1.85 – 1.81 (m, 2H). **^{13}C NMR** (126 MHz, methanol-d_4) δ 74.00, 72.24, 64.53.

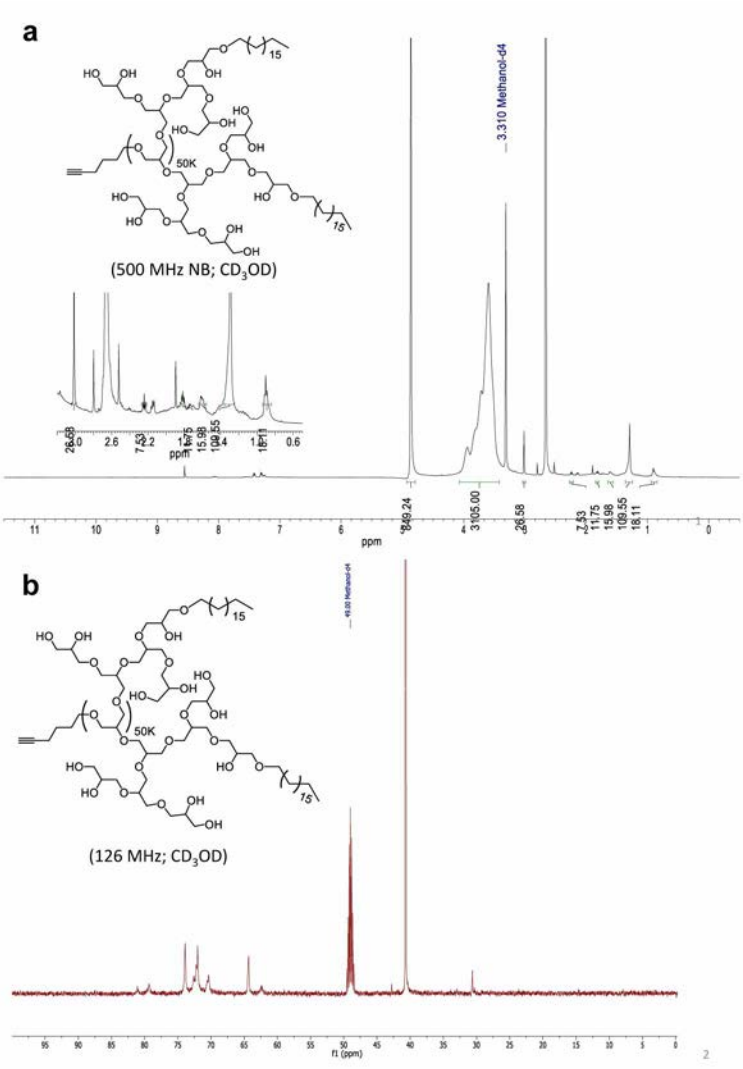

Figure S11. Characterization of HPG_{50k}-g-C_{18}(2) by **(a)** ^{1}H NMR and **(b)** ^{13}C NMR. Protons of the C_{18} chain are from 1-2 ppm in the ^{1}H NMR spectrum. HPG_{50k}-g-C_{18}(2) represents HPG (MW ~50,000 g/mol) substituted with 2 C_{18} chains. **^{1}H NMR** (500 MHz, methanol-d_4) δ 4.88 (s, 849H), 4.10 – 3.37 (m, 3105H), 3.03 (d, J = 3.0 Hz, 26H), 2.26 (t, J = 7.3 Hz, 8H), 1.88 – 1.78 (m, 12H), 1.67 – 1.56 (m, 16H), 1.32 (d, J = 9.5 Hz, 110H), 0.91 (dt, J = 10.0, 6.0 Hz, 18H). **^{13}C NMR** (126 MHz, methanol-d_4) δ 78.69, 72.84, 71.25, 71.04, 69.49, 63.36, 47.91, 47.84, 47.74, 47.56, 47.45, 47.39, 41.44, 39.28, 29.59.

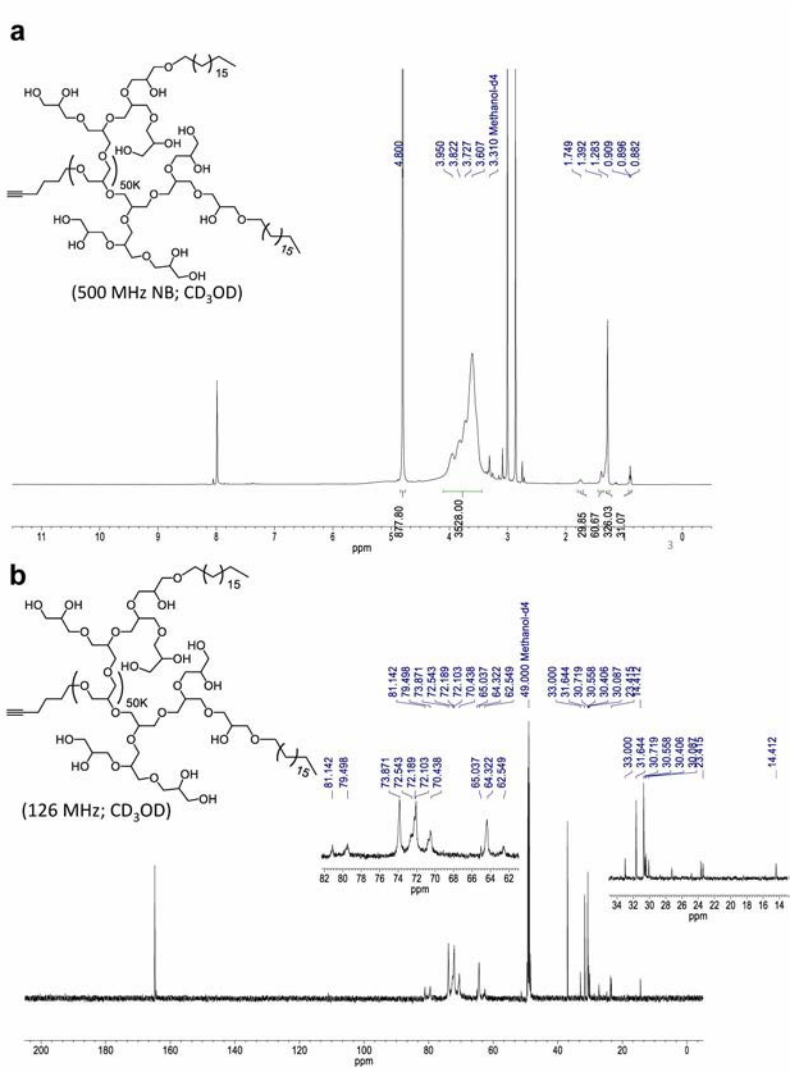

Figure S12. Characterization of HPG_{50k}-g-C_{18}(10) by **(a)** ^{1}H NMR and **(b)** ^{13}C NMR.

Protons of the C_{18} chain are from 1-2 ppm in the ^{1}H NMR spectrum. HPG_{50k}-g-C_{18}(10) represents HPG (MW ~50,000 g/mol) substituted with 10 C_{18} chains. **^{1}H NMR** (500 MHz, methanol-d_4) δ 4.80 (s, 878H), 3.95 – 3.61 (m, 3528H), 1.75 (dd, J = 10.9, 5.9 Hz, 30H), 1.40 (d, J = 5.7 Hz, 60H), 1.28 (s, 326H), 0.91 (t, J = 6.7 Hz, 31H). **^{13}C NMR** (126 MHz, methanol-d_4) δ 81.14, 79.50, 73.87, 72.54, 72.19, 72.10, 70.44, 65.04, 64.32, 62.55, 30.00, 31.64, 30.72, 30.56, 30.41, 30.09, 23.42, 14.41.

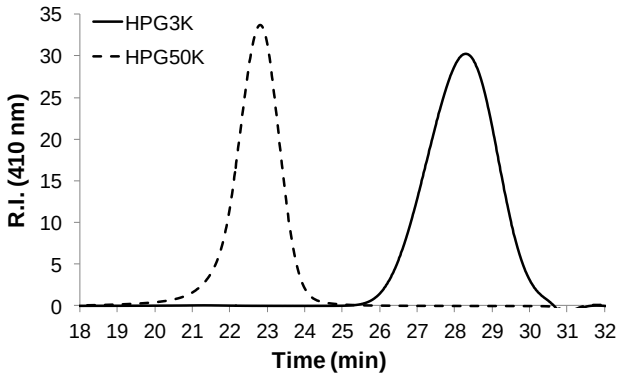

Compounds Synthesized	SEC DMF MW [a]	PDI
HPG_{3k}	28.28 min (3019 MW)	1.20
HPG_{50k}	22.80 min (46,025 MW)	1.46

[a] PEG standards

Figure S13. Characterization of molecular weights of HPG_{3k} and HPG_{50k} by GPC. The molecular weight of HPG_{3k} is in agreement with that determined by MALDI-TOF.

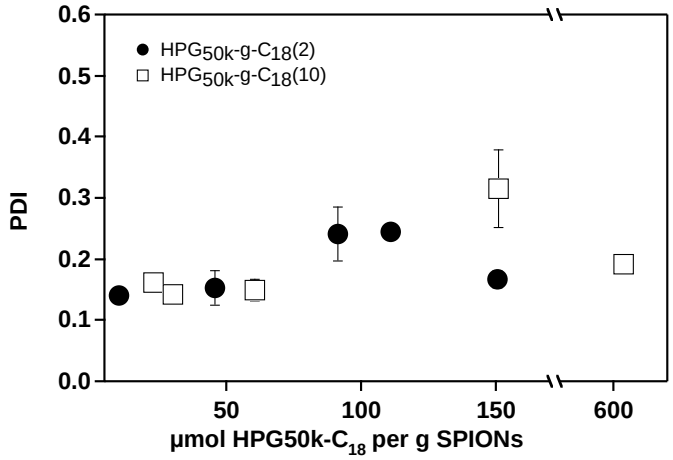

Figure S14. Polydispersity index (PDI) for the size-tunable clusters shown in Figure 2 of the text. Data are the average of three replicate measurements, with error bars representing standard deviation partially obscured by data point markers.

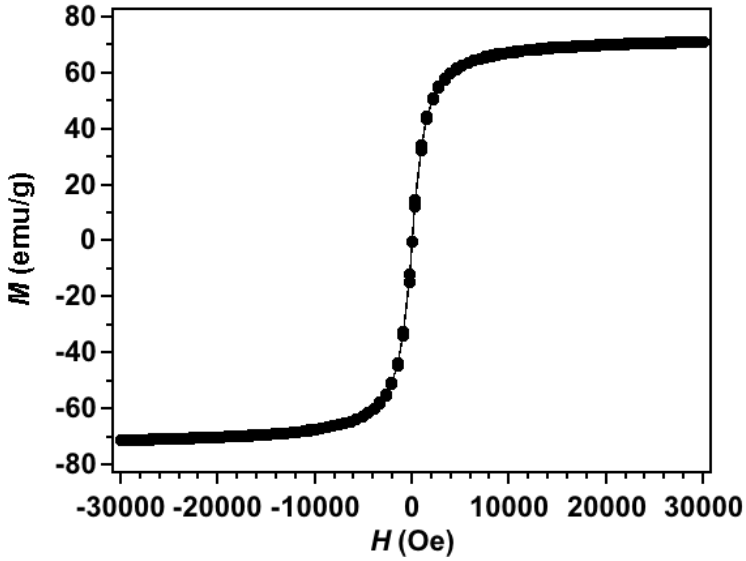

Figure S15. Magnetization curve of oleic acid-capped SPIONs at 300 K. A saturation magnetization, M_s, of 71 emu/g, determined from the plateau of the magnetization curve, was used to estimate theoretical maximum relaxivity in Eq. (3) of the text.

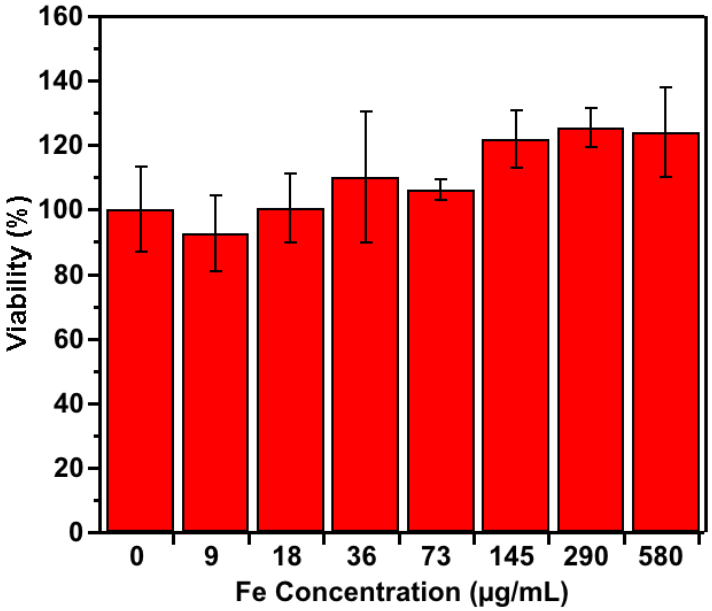

Figure S16. MTT assay to assess effects of HPG-SPION nanoclusters on metabolic activity of C166 endothelial cells. Percent viability was determined by normalization of absorbance values after blank subtraction to that of a control group of cells incubated without HPG-SPIONs. The concentration of Fe in the cell culture media was varied by altering the mass of SPION clusters. Values are the average of 3 replicates and error bars represent standard deviation.

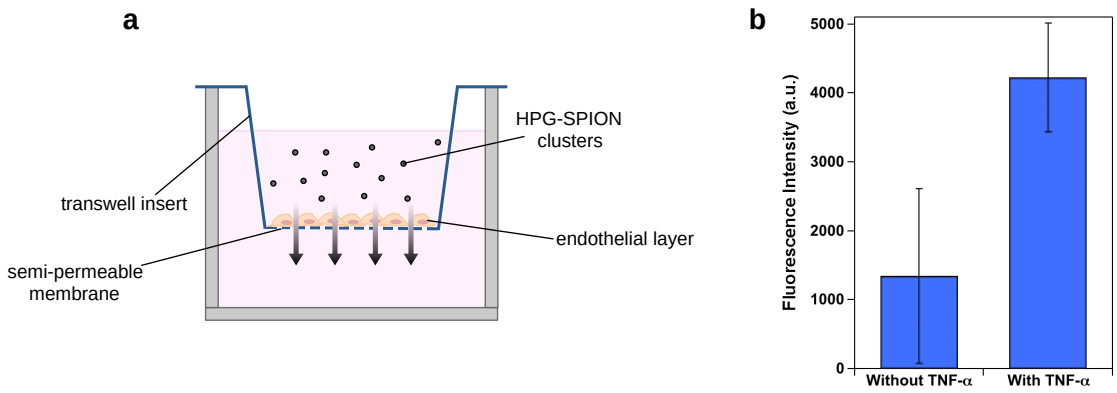

Figure S17. Endothelial transwell migration assay. **(a)** Schematic of the transwell insert. **(b)** Fluorescence intensity of the receiving well after incubation of FITC-labeled HPG-SPIONs and C166 cells with and without exposure to inflammation-inducing TNF-α. The diffusion of HPG-SPION nanoclusters was more than 3-fold higher through the endothelial layer exposed to TNF-α. Error bars represent standard deviation of three replicates.

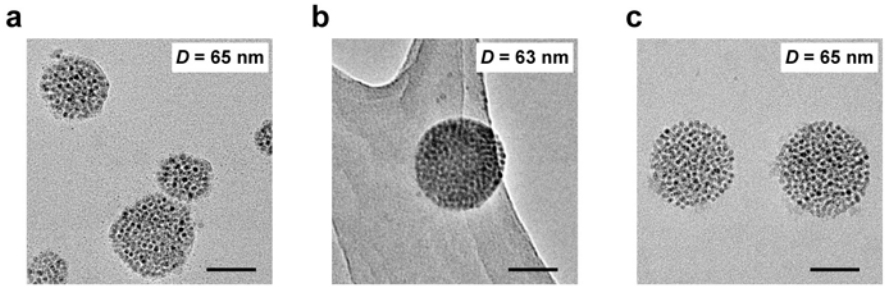

Figure S18. TEM micrographs of HPG-SPIONs before and after incubation with 50% human serum in PBS. The HPG-SPIONs with a hydrodynamic diameter of 122 nm and relaxivity of 719 $mM^{-1}s^{-1}$ were analyzed, and average core diameter is indicated on each figure. **(a)** TEM and **(b)** cryo-TEM images of the SPION clusters before serum incubation. **(c)** After incubation with 50% human serum in PBS for 2 h at 37 °C, the morphology and size remained unchanged, according to TEM micrographs. Scale bars represent 50 nm.

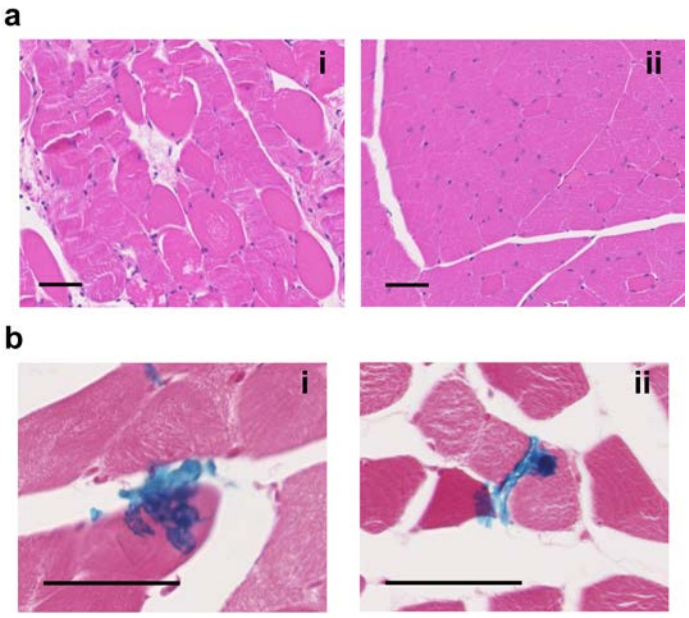

Figure S19. Histological analysis of the hindlimb ischemia model. **(a)** H&E staining of (i) the thigh of the ischemic left hindlimb, indicating tissue damage as a result of ischemia and (ii) the thigh of the uninjured, right hindlimb. **(b)** Prussian blue staining of the left, ischemic hindlimb sections containing (i) HPG-SPION nanoclusters and (ii) unclustered SPIONS, indicating the presence of contrast agent in both cases. In all figures, scale bars represent 50 μm.